

Removal of Heavy Metals by Bacteria in Bio-Ceramsite and their Toxicity to Bacteria

YAN SHI^{1,2}, XUEBIN QI^{1,*} and QING GAO¹

¹Farmland Irrigation Research Institute, Chinese Academy of Agricultural Sciences, Xinxiang 453002, P.R. China

²North China University of Water Resources and Electric Power, Zhengzhou 450011, P.R. China

*Corresponding author: E-mail: shiyan@ncwu.edu.cn, yanshichem@sohu.com

Received: 30 April 2014;

Accepted: 13 July 2014;

Published online: 30 March 2015;

AJC-17057

Heavy metal pollution has become one of the global environmental pollution problems of concern. Bio-ceramsite technology is one of the most effective technologies in pretreatment of drinking water. This technology can be employed to remove heavy metals and organic pollutants from water. In this paper, Pb(II) and Cd(II) adsorption by the bio-ceramsite with *Citrobacter freundii* (*C. freundii*) immobilization was studied. The findings of the current study suggest that the bio-ceramsites showed biosorption abilities for Cd(II) and Pb(II) and the removal efficiency for Pb(II) is lower than Cd(II). The adsorption mechanism can be attributed to electrostatic attraction and covalent bond. The morphology of the cells changed after the adsorption of Cd(II) and Pb(II) due to the dissociation of the assembly of peptidoglycan and lipopolysaccharide. The fluorescence polarization has shown a significant decrease in membrane fluidity and the increase of permeability of cell membrane. The spectral profile of *C. freundii* suggests the alteration of carbonyl, amide and phosphonic group on the cell membrane.

Keywords: Immobilization, Biosorption, Bio-ceramsite, Dissociation, Cell membrane.

INTRODUCTION

Heavy metal pollution is a typical representation of environmental problem because of the toxic effects of metals, which can damage nerves, liver, bones and block functional groups of vital enzymes and their accumulation throughout the food chain leads to serious ecological and health problems. These toxic metal ions are generated from mining operations, metal plating facilities, power generation facilities, electronic device manufacturing units and tanneries and commonly existed in process waste streams, which has been increased dramatically during the last few decades in ambient environment¹⁻⁴. Thus, the removal of such toxic metal ions from effluent is a crucial issue.

Most heavy metal salts can dissolve in the water and form aqueous solutions, as a consequence, cannot be separated by general physical separation methods. Physico-chemical methods such as chemical precipitation, chemical oxidation or reduction, electrodeposition and electrocoagulation, solvent exchange and membrane separation technologies have been widely used to remove heavy metal ions from industrial wastewater^{5,6}. But these processes may be ineffective or expensive, especially when the heavy metal ions are in solutions containing in the order of 1-100 mg dissolved heavy metal ions^{7,8}. Biological methods for the removal of heavy metal ions may provide an attractive alternative to physico-chemical methods.

Many of them have been used in different aspects, including removal of Cr(VI) in wastewater by fungi, removal of chromium from aqueous solution using mixture of *Candida lipolytica* and dewatered sewage sludge and removal of sulfate and copper by a PVA-immobilized sulfate reducing bacterial⁹.

Bio-ceramsite technology is one of the most effective technologies in pretreatment of drinking water¹⁰⁻¹². This technology can be employed to remove heavy metals and organic pollutants from water. The structure of porous ceramsite is complicated. It has been reported that the porous structure of sludge-ceramsite improves the mass transfer efficiencies. Generally, adsorption is the major mechanism accounting for the removal of heavy metals and organic pollutants by bio-ceramsite. It has also been demonstrated that, with the microorganism reproduction on the ceramsite surface which promoted ceramsite aging, the organic pollutant removal is due to the combined action of adsorption and bio-degradation. The pollutant removal efficiency is directly affected by adsorption capacities of ceramsite materials, which depend on their various structural characteristics. A multiplex porous structure can be formed on the ceramsite surface after alkaline hydrothermal reaction, which could obviously increase the superficial area and absorption efficiency. Bacteria can also adsorb considerable amount of aqueous metal cations because of charged organic acid functional groups. Several studies have proposed that electric double-layer interaction on the bacterial surface plays an important

role in proton and metal binding. And different surface electric field models have been adopted to account for these effects.

Therefore, both bacteria and ceramsite can be used to remove toxic metals from contaminated wastewater and industrial effluents. So to improve the pollutant removal efficiency and the material reusability is a critical issue. So far, there is no report about the effectiveness of the combination of bacteria and ceramsite. It looks promising to study the co-effect of bacteria and ceramsite and their potential applications in removing toxic metals from sewage sludge.

In the bio-ceramsite technology for heavy metal removal, bacteria are generally absorbed in ceramsite first and then heavy metals are absorbed by the bacteria immobilized ceramsite. To clarify the roles of the micropore structure of ceramsite and bacteria in removing heavy metals, *C. freundii* was chosen as the model bacterium to be immobilized on the ceramsite in this study. *C. freundii* is known for its capability to absorb metal ions. Additionally *C. freundii* has evolved a set of strategies that allow survival under harsh conditions. To study the adsorption capacity of *C. freundii* in wastewater purification, the amount of adsorbed heavy metal ions was measured and the morphology was observed by scanning electron microscopy (SEM). Alteration of the molecular groups on bacteria was also analyzed and the toxicity of the adsorbed heavy metal ions to bacteria was measured.

EXPERIMENTAL

C. freundii was provided by the Chinese Center for Type Culture Collections. All chemicals were analytical grade. The medium contained NaCl 5 g, peptone 5 g, beef extract 5 g and yeast extract 6 g per 1000 mL (pH = 7.2). The medium was sterilized in high-pressure steam at 120 °C for 0.5 h.

CdCl₂ and Pb(NO₃)₂ were purchased from Sigma-Aldrich, MO, U.S.A. Deionized and doubly distilled water was used in all experiments. Bio-ceramsite was provided by Harbin Institute of Technology.

Immobilization of *C. freundii* on the ceramsite: The immobilization of *C. freundii* cells on the ceramsite was evaluated at the desired pH with 1.5 g/L *C. freundii* suspension. Distilled water was used as the supporting electrolyte. 0.5 g ceramsite was taken into a 100 mL Bunsen beaker which contained 50 mL *C. freundii* suspension and the suspension was stirred for 10 min with a magnetic stirrer at 400 rpm. After full adsorption, the suspension was filtered with perforated sieve to separate the ceramsite from solution. The quantity of unabsorbed *C. freundii* in solution was determined by spectrophotometer and the corresponding bacteria concentration was obtained through normal bacterial calibration curve.

Heavy metals adsorption: Pb(II) and Cd(II) were used separately to evaluate the adsorption capacity of the ceramsite with *C. freundii* immobilization. Each test was performed with 400 µg/mL metal ion solution containing bio-ceramsite samples, which was continuously shaken for 3 days at room temperature. The mixture was then centrifuged at 3000 rpm for 4 min. The metal concentrations in the supernatant were analyzed by an Inductively Coupled Plasma-Atom Emission Spectrometry (ICP-AES) (Optima 3000, Perkin-Elmer, USA).

SEM observation: After the full adsorption and treatment, the perforated sieve was used to separate the immobilized ceramsite from solution. The ceramsite was then washed by pure water three times. The cells were desorbed from the ceramsite by continuous shaking in 1 % KCl solution for 24 h. Glutaraldehyde and osmium tetroxide were used to fix and dehydrate the protein (or lipid) in cells. Double fixation by oxidation after reduction made the most of the characteristics of two different fixatives. Then the cells were dehydrated in a series of increasing concentration of ethanol (50, 60, 70, 80, 90, 95 and 100 %). After the cells were fixed and dehydrated, they were observed by SEM (HITACHI, S-4800).

Analysis of cell surface hydrophobicity: The bacterial adhesion to xylene was used to test the cell surface hydrophobicity of the strains. All isolates were grown (100 mL) in a 250 mL Erlenmeyer flask in a rotary shaker at 130 rpm and 30 °C. Bacterial cells were harvested by centrifugation for 10 min, washed twice in sterile phosphate-buffered (pH = 7.1). Then the cells were suspended in the same buffer with an initial optical density (OD) at 600 nm. Cells (3 mL of microbial suspension) and 300 mL of xylene were mixed and vortex for 1 min. After vortexing, the xylene and the aqueous phases were allowed to separate for 45 min. The aqueous phase was carefully removed and the OD (A₁) determined at 600 nm. Hydrophobicity was expressed as the percentage of cell adherence to xylene, which is calculated as follows:

$$[1-(A_1/A_0)] \times 100$$

Fluorescence polarization method: Bacterial cells from a 24 h culture were aseptically harvested by centrifugation at 5000 rpm for 5 min and washed twice in sterile 15 mM tris-HCl buffer (pH 7) and resuspended in the same buffer to an optical density 600 nm of 0.4. One microliter of the fluorescent membrane probe, 1,6-diphenyl-1,3,5-hexatriene (DPH, Molecular Probes, Eugene, Oregon, USA) (12 mM stock solution in tetrahydrofuran), was added to 3 mL of each resuspended culture in a quartz cuvette and incubated for 10 min in the dark at room temperature to allow probe incorporation into the cytoplasmic membrane.

Fluorescence polarization was measured using a spectrofluorometer (Photon Technology International Inc., London, ON, Canada) equipped with a temperature-controlled cuvette holder and a magnetic cuvette stirrer. Excitation and emission wavelengths were set at 358 and 428 nm, respectively. Polarizers were set in either a vertical or a horizontal position. The slit widths for the excitation and emission beams were 5 and 10 nm, respectively. Voltages for the horizontal and vertical polarized light amplifiers were 1002 and 1031 V, respectively. Data were recorded using FELIX software (Version 1.4, Photon Technology International). The degree of polarization (P, unitless) was calculated from the emission fluorescence intensities measured parallel and perpendicular.

ATR-FTIR spectra: ATR-FTIR spectra were measured in a Portmann Instruments AG spectrophotometer equipped with a specac attachment (45° one pass diamond crystal). Spectra were the results of 256 scans with a resolution of 2 cm⁻¹ in the spectral range 4000-500 cm⁻¹. Specimens for ATR-FTIR were prepared by two different techniques: 0.5 mL of the liquid from the batch reactor was evaporated on the microscope glass.

RESULTS AND DISCUSSION

Removal of Cd(II) and Pb(II): Fig. 1 shows the isotherm curves for the removal of Cd(II) and Pb(II) in Fig. 1a and b, respectively. The metal removal rate is rapid, especially in the first few minutes. The aqueous metal concentrations decreased in the first 5 h and then slowly increased in the next 30 h.

This is particularly true for strain Cd(II). For instance, its removal efficiency for the solution with an initial concentration of 5 mg/L is around 56 % in 2 h; 65 % in 10 h, 67 % in 30 h. For Pb(II), its removal efficiency with an initial concentration of 5 mg/L is around 7.5 % in 2 h; 21 % in 10 h, 27 % in 30 h. The removal efficiency for Pb(II) is lower than Cd(II) evidently.

Electrostatic attraction played an important role in metal ion adsorption^{13,14}. The ceramsite built on the basis of the ionization degree with SiOH groups on the surface is characterized with negative charges. The bacteria surface also has the negative charges. The metal ions with positive charges could be adsorbed by both *C. freundii* and ceramsite. The size of Cd(II) is smaller than Pb(II), which is in favor of electrostatic attraction. It should be noted that the electrostatic attraction is not the unique force between metal ions and solid surface. The covalent bond plays an important role in the process of adsorption. The covalent bond derives from the affinity of metal ions for the N-, O-, C-, especially -SH, terminals on the surface of bacteria and -OH on the ceramsite surface. Compared with

Pb(II), Cd(II) has valence electrons in *d*-orbital, which is easier to bind with non-metallic element. In the chemical interaction occurring between bacteria and metal ions, Cd(II) is easier than Pb(II) to form coordination compound, whose lone pair electrons are offered by O, N, P atoms on bacterial surface. As a result, Cd(II) is more easily absorbed on the bio-ceramsite surface and the removal efficiency improved.

SEM image for *C. freundii* after the adsorption of Cd(II) and Pb(II): In this study, the surface changes of *C. freundii* cell were investigated by FE-SEM. The microstructures of the three samples were obtained, as shown in Fig. 2. In Fig. 2(A), SEM image revealed that the surface structure of the native *C. freundii* was almost intact, with regular wrinkles. Fig. 2(B) shows the image of the *C. freundii* cell adsorbed by Pb(II). The morphological character of the cells also changed, for example, the cells bulged at two ends and became wider and shorter. As for Fig. 2(C), the cells after adsorption with Cd(II) were almost completely deformed. The cells became twisted and rougher. The normal cell kept rod shape while some cells after treatment became elliptical.

The outer membrane of the negative bacteria is composed of lipopolysaccharide, peptidoglycan and periplasm. The strength of cell wall depends largely on peptidoglycan, whose structure is a mechanically strong network¹⁵. Thus, the cell wall, firm and resilient as it is, plays an important role in the maintenance of cell morphology. During adsorption, heavy

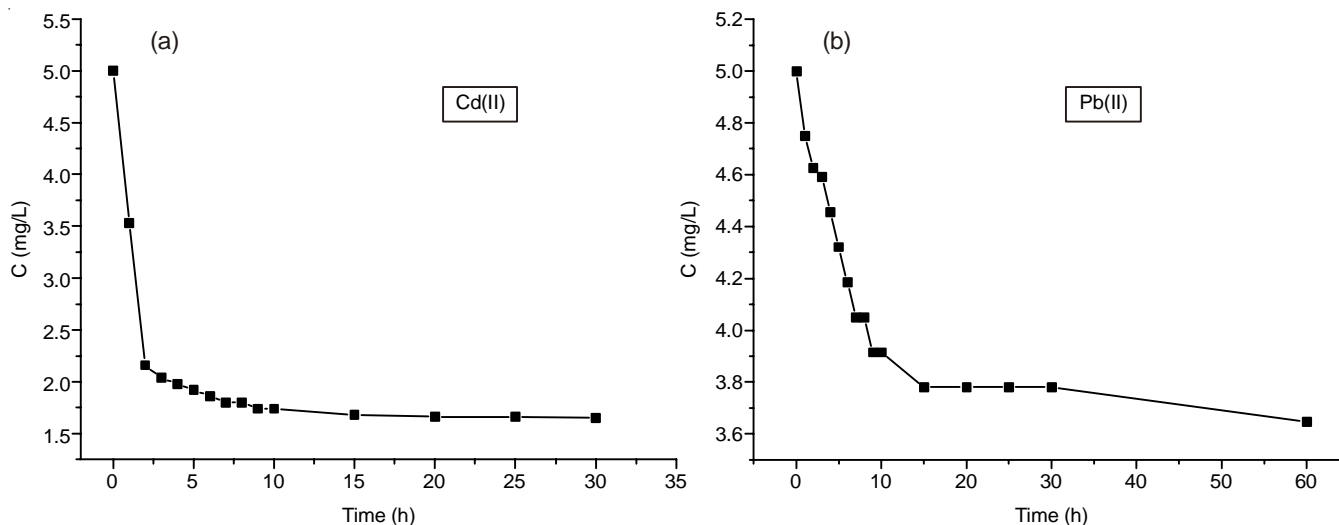


Fig. 1. Dynamic process of adsorption in ceramsite for Cd(II) and Pb(II)

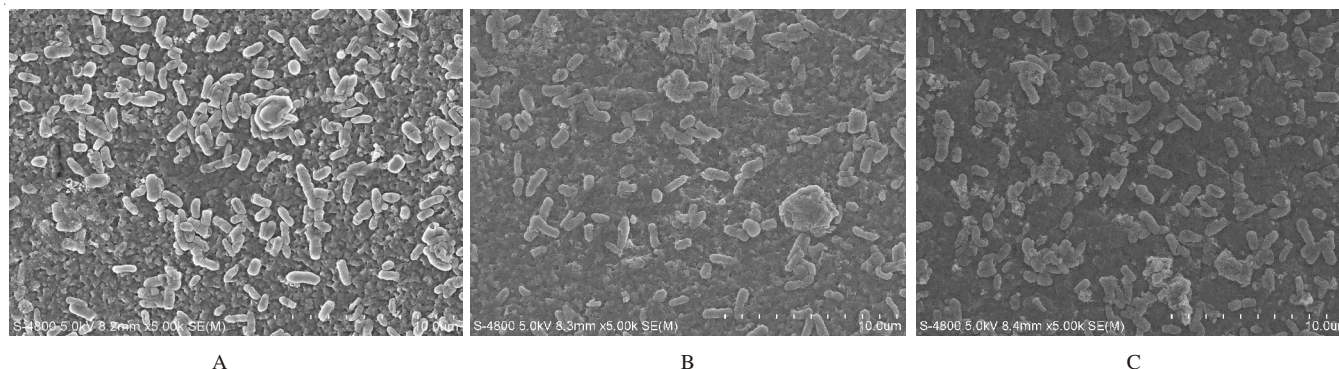


Fig. 2. SEM images of the native *C. freundii* cells (A) and the cells after adsorption for Pb(II) (B) and Cd(II) (C)

metal ions could enter the assembly of peptidoglycan and lipopolysaccharide, which are bacterial cell wall components. The binding sites of Gram negative bacterial for enrichment of heavy metal ions mainly are the phosphate group of the polysaccharide and N-acetylglucosamine residues on oligosaccharide. After the adsorption of metal ion, the morphological character of the cells has changed, for example two end of cell bulged for the reason that the cell wall were partially eliminated. It indicated that the presence of metal ions in facilitates dissociation of lipopolysaccharide, peptidoglycan and periplasm from the assembly. The cell wall couldn't work as the protecting shell effectively.

Change of cell surface hydrophobicity: The alteration of the cell surface hydrophobicity was listed in Table-1. The cell surface hydrophilicity increased after adsorption of metal ions. The cells absorbed by Cd(II) is more hydrophilic than by Pb(II). It is easy to understand that after metal ions enter the assembly composed by biological macromolecules, the molecular polarity and the hydrophilicity will increase.

The absorption can enhance the adherence to the ceramsite surface, since this material is hydrophilic under normal conditions. In general, hydrophobic bacteria adhere on hydrophobic surfaces, whereas hydrophilic ones prefer hydrophilic surfaces¹⁶.

	Native cells	Cells absorbed by Pb(II)	Cells absorbed by Cd(II)
Cell surface hydrophobicity	28.53	24.32	21.68

Membrane fluidity of the cells: The 1,6-diphenyl-1,3,5-hexatriene fluorescent probe was easily incorporated into the cytoplasmic membrane without disrupting the intact cells and membrane. The probe does not interfere with the event being measured, no pretreatment of cells was necessary and a high polarization value indicates high structural order or low membrane fluidity. The membrane polarization values reported in this study for the five bacteria are considered normal values for cytoplasmic membranes at the specific temperatures and growth conditions^{17,18}.

1,6-Diphenyl-1,3,5-hexatriene (DPH) polarization reflects the average fluidity of all cellular membrane lipids and an inverse relationship exists between membrane fluidity and polarization. In our study, both Cd(II) and Pb(II) caused an increase in the fluorescence polarization of 1,6-diphenyl-1,3,5-hexatriene (Fig. 3). It reflects a significant decrease in membrane fluidity. Accordingly, the permeability of cell membrane would increase.

Spectral profile of cell surface: As can be seen from Fig. 1, the ATR-FTIR spectra of *C. freundii* vary after the metal adsorption in the fingerprint region with time. The profile of polysaccharide bands were observed to change significantly after adsorption. In the C-O-C glycosidic linkage region 1029 cm^{-1} disappear. The intensity decrease of the broad 1140-1000 cm^{-1} band was detected^{19,20}. The external bilayer of the asymmetric outer membrane is composed only of amphipatic molecules, the lipo-polysaccharides. This makes it possible to relate the observed spectral changes to lipo-polysaccharide damage.

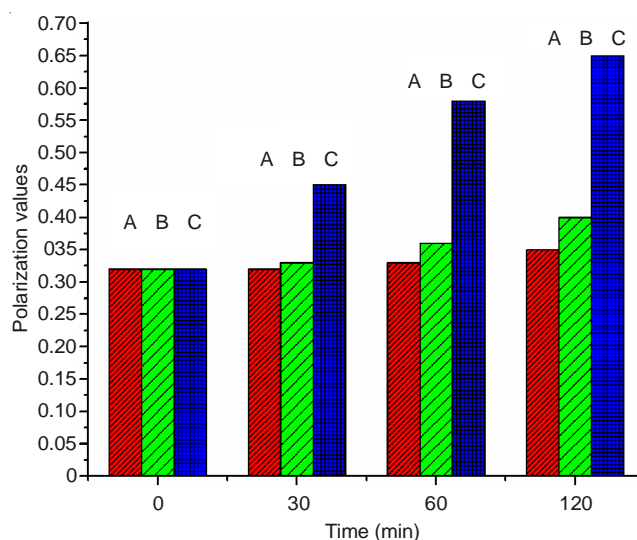


Fig. 3. Polarization value of cells with different adsorption time for the native *C. freundii* (A) and the cells after adsorption for Pb(II) (B) and Cd(II)(C)

The carbonyl group absorbance between 1700 and 1500 cm^{-1} changed considerably in the ATR-FTIR spectra. A raise in the peak intensities at 1639 cm^{-1} and at 1538 cm^{-1} were readily detected. A concomitant increase in the absorption shoulder at 2923 cm^{-1} also occurred. The observed carboxy group during adsorption process appears near 1400 cm^{-1} and corresponds to the O-C-O symmetric stretching vibrations. The decrease of the peak at 1639 cm^{-1} stands for the breaking of the acyl-bond in lipids. Significant changes in the profile of PO_2^- bands were observed in the spectral range 1280-1200 cm^{-1} . Band profiles of PO_2^- are sensitive to the hydration-dehydration of the phosphonic groups and this taken as an indicator for the structural organization of lipids²¹. The amide I band (s) was observed to vary during the adsorption in Fig. 4 providing the evidence for the protein conformational changes²². Changes in the spectral profile for the decrease in amide I 1639 cm^{-1} , II 1538 cm^{-1} and for the significant decay of amide A 3290 cm^{-1} were observed, which suggests the outer leaflet damage of amide groups.

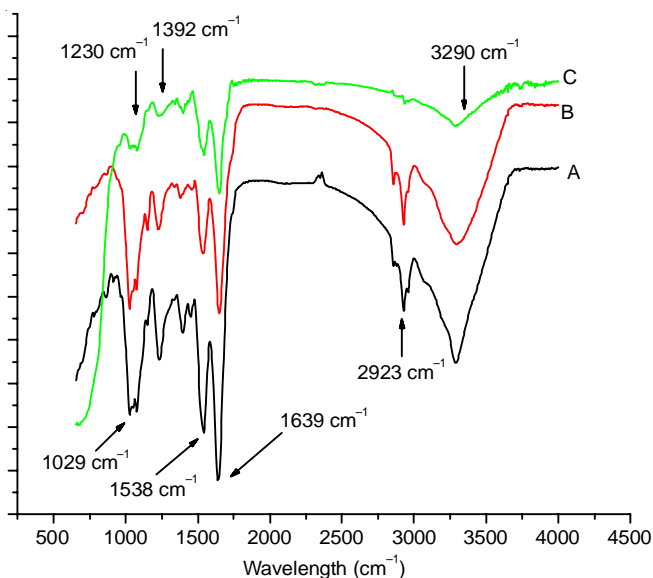


Fig. 4. ATR-FTIR spectra of for the native *C. freundii* (A) and the cells after adsorption for Pb(II) (B) and Cd(II)(C)

Conclusion

The findings of the current study showed bio-ceramites have increased biosorption abilities for Cd(II) and Pb(II). The removal efficiency for Pb(II) is lower than Cd(II) evidently. The mechanism can be attributed to electrostatic attraction and covalent bond. Heavy metal ions could enter the assembly of peptidoglycan and lipopolysaccharide, which are bacterial cell wall components. As a result, the bio-macromolecular assembly was dissociated on the cell surface. The morphological character of the cells changed after the adsorption of Cd(II) and Pb(II). The fluorescence polarization has shown a significant decrease in membrane fluidity and the increase of permeability of cell membrane. The spectral profile of *C. freundii* suggests the alteration of carbonyl, amide and phosphonic group on the cell membrane.

ACKNOWLEDGEMENTS

Funded by the National High Technology Research and Development Program of China (863 Program): the key technologies of degraded soil restoration and Wastewater irrigation farmland(2012AA100604)

REFERENCES

1. C.N. Mulligan, R.N. Yong and B.F. Gibbs, *Eng. Geol.*, **60**, 193 (2001).
2. L. Järup, *Br. Med. Bull.*, **68**, 167 (2003).
3. V.J. Camobreco, B.K. Richards, T.S. Steenhuis, J.H. Peverly and M.B. McBride, *Soil Sci.*, **161**, 740 (1996).
4. V.L. Colin, L.B. Villegas and C.M. Abate, *Int. Biodeterior. Biodegrad.*, **69**, 28 (2012).
5. H. Hussein, S. Farag and H. Moawad, *Arab J. Biotechnol.*, **7**, 13 (2004).
6. H. Hussein, S. Farag Ibrahim, K. Kandeel and H. Moawad, *Electron. J. Biotechnol.*, **7**, 38 (2004).
7. N. Meunier, J. Laroulandie, J.F. Blais and R.D. Tyagi, *Bioresour. Technol.*, **90**, 255 (2003).
8. B. Volesky and Z.R. Holan, *Biotechnol. Prog.*, **11**, 235 (1995).
9. H.D. Li, T. Liu, Z. Li and L. Deng, *Bioresour. Technol.*, **99**, 2234 (2008).
10. G. Ahlberg, O. Gustafsson and P. Wedel, *Environ. Pollut.*, **144**, 545 (2006).
11. J.Q. Sang, X.H. Zhang, L.Z. Li and Z.S. Wang, *Water Res.*, **37**, 4711 (2003).
12. A. Fullana, J.A. Conesa, R. Font and S. Sidhu, *Environ. Sci. Technol.*, **38**, 2953 (2004).
13. D.A. Ams, J.S. Swanson, J.E.S. Szymanowski, J.B. Fein, M. Richmann and D.T. Reed, *Geochim. Cosmochim. Acta*, **110**, 45 (2013).
14. C. Liu, C. Duan, J. Zhou, X. Li, G. Qian and Z.P. Xu, *Appl. Clay Sci.*, **75-76**, 39 (2013).
15. L.S. Chen and W.G. Coleman Jr., *J. Bacteriology*, **175**, 2534 (1993).
16. P.K. Sharma and K. Hanumantha Rao, *Adv. Colloid Interface Sci.*, **98**, 341 (2002).
17. J.T. Trevors, *J. Biochem. Biophys. Methods*, **57**, 87 (2003).
18. T.J. Denich, L.A. Beaudette, M.B. Cassidy, H. Lee and J.T. Trevors, *J. Fluorescence*, **13**, 385 (2003).
19. D. Naumann, C. Schultz, A. Sabisch, M. Kastowsky and H. Labischinski, *J. Mol. Struct.*, **214**, 213 (1989).
20. Kacurakova and M. Mathlouthi, *Carbohydr. Res.*, **284**, 145 (1996).
21. R. Kinder, C. Kinder, J.M. Kinder, *Int. J. Radiat. Biol.*, **71**, 561 (1997).
22. D. Naumann, *Appl. Spectrosc. Rev.*, **36**, 239 (2001).